Since antiquity, humans have wondered whether our Universe is finite or infinite. Now, after more than two millennia of speculation, observational data might finally settle this ancient question. □

Received 23 June; accepted 28 July 2003; doi:10.1038/nature01944.

1. Bennett, C. L. *et al.* First year Wilkinson Microwave Anisotropy Probe (WMAP 1) observations: Preliminary maps and basic results. *Astrophys. J. Suppl.* **148,** 1–27 (2003).
2. Spergel, D. N. *et al.* First year Wilkinson Microwave Anisotropy Probe (WMAP 1) observations: Determination of cosmological parameters. *Astrophys. J. Suppl.* **148,** 175–194 (2003).
3. Contaldi, C. R., Peloso, M., Kofman, L. & Linde, A. Suppressing the lower multipoles in the CMB anisotropies. *J. Cosmol. Astropart. Phys.* **07,** 002 (2003).
4. Cline, J. M., Crotty, P. & Lesgourgues, J. Does the small CMB quadrupole moment suggest new physics? *J. Cosmol. Astropart. Phys.* (in the press); preprint at ⟨http://arXiv.org/astro-ph/0304558⟩ (2003).
5. Efstathiou, G. Is the low CMB quadrupole a signature of spatial curvature? *Mon. Not. R. Astron. Soc.* **343,** L95–L98 (2003).
6. Tegmark, M., de Oliveira-Costa, A. & Hamilton, A. A high resolution foreground cleaned CMB map from WMAP. *Phys. Rev. D* (in the press); preprint at ⟨http://arXiv.org/astro-ph/0302496⟩ (2003).
7. Cornish, N., Spergel, D. & Starkman, G. Circles in the sky: Finding topology with the microwave background radiation. *Class. Quant. Grav.* **15,** 2657–2670 (1998).
8. Uzan, J.-P., Kirchner, U. & Ellis, G. F. R. WMAP data and the curvature of space. *Mon. Not. R. Astron. Soc.* (in the press).
9. Linde, A. Can we have inflation with $\Omega > 1$? *J. Cosmol. Astropart. Phys.* **05,** 002 (2003).
10. Lehoucq, R., Weeks, J., Uzan, J.-P., Gausmann, E. & Luminet, J.-P. Eigenmodes of 3-dimensional spherical spaces and their application to cosmology. *Class. Quant. Grav.* **19,** 4683–4708 (2002).
11. Gausmann, E., Lehoucq, R., Luminet, J.-P., Uzan, J.-P. & Weeks, J. Topological lensing in spherical spaces. *Class. Quant. Grav.* **18,** 5155–5186 (2001).
12. Riazuelo, A., Uzan, J.-P., Lehoucq, R. & Weeks, J. Simulating cosmic microwave background maps in multi-connected spaces. *Phys. Rev. D* (in the press); preprint at ⟨http://arXiv.org/astro-ph/0201222⟩ (2002).

Acknowledgements J.R.W. thanks the MacArthur Foundation for support.

Competing interests statement The authors declare that they have no competing financial interests.

Correspondence and requests for materials should be addressed to J.R.W. (weeks@northnet.org).

Fermi-liquid breakdown in the paramagnetic phase of a pure metal

N. Doiron-Leyraud[1], **I. R. Walker**[1], **L. Taillefer**[2], **M. J. Steiner**[1], **S. R. Julian**[1] **& G. G. Lonzarich**[1]

[1]*Cavendish Laboratory, University of Cambridge, Cambridge CB3 0HE, UK*
[2]*Département de Physique, Université de Sherbrooke, Québec J1K 2R1, Canada*

Fermi-liquid theory[1] (the standard model of metals) has been challenged by the discovery of anomalous properties in an increasingly large number of metals. The anomalies often occur near a quantum critical point—a continuous phase transition in the limit of absolute zero, typically between magnetically ordered and paramagnetic phases. Although not understood in detail, unusual behaviour in the vicinity of such quantum critical points was anticipated nearly three decades ago by theories going beyond the standard model[2–5]. Here we report electrical resistivity measurements of the 3*d* metal MnSi, indicating an unexpected breakdown of the Fermi-liquid model—not in a narrow crossover region close to a quantum critical point[6,7] where it is normally expected to fail, but over a wide region of the phase diagram near a first-order magnetic transition. In this regime, corrections to the Fermi-liquid model are expected to be small. The range in pressure, temperature and applied magnetic field over which we observe an anomalous temperature dependence of the electrical resistivity in MnSi is not consistent with the crossover behaviour widely seen in quantum critical systems[8,9,31]. This may suggest the emergence of a well defined but enigmatic quantum phase of matter.

In the investigation of anomalous metallic properties, often referred to as non-Fermi-liquid phenomena, complications of various types may arise that can lead to ambiguous interpretations. These can be related, for example, to band structure anomalies, to magneto-crystalline anisotropies, to the effective dimensionality or to disorder effects. In other materials, the emergence of superconductivity may make it difficult to probe the fundamental nature of the normal state of the underlying electronic system. In order to conclusively assess and clarify our ideas about non-Fermi-liquid phenomena in metals, it is essential to study materials that fulfil the desirable criteria of purity, simplicity and convenience. The itinerant-electron ferromagnet MnSi appears to be one such example[10]. Under ambient conditions of pressure and applied magnetic field, MnSi orders ferromagnetically with a small average moment of up to 0.4 μ_B per Mn atom (where μ_B is the Bohr magneton) and a Curie temperature T_C of 29.5 K (ref. 11). At low temperatures, it exhibits properties consistent with the formation of a weakly spin-polarized Fermi liquid dominated by moderately renormalized 3*d* bands. With its full three-dimensional cubic crystal structure, the electronic and magnetic properties of MnSi are essentially isotropic, except for the effects of a well-understood long-wavelength helical twist of the ferromagnetic order characteristic of crystalline structures lacking inversion symmetry—such as the B20 lattice of MnSi (ref. 12).

The possibility of producing ultra-pure single crystals of MnSi

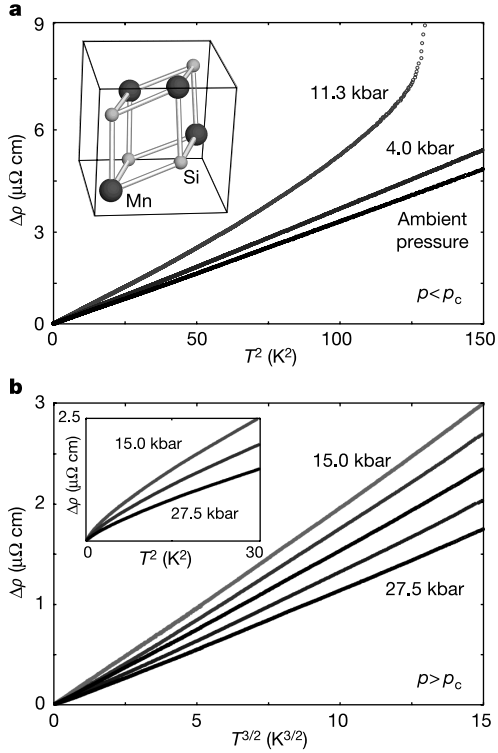

Figure 1 Dependence on temperature of the electrical resistivity of MnSi. The temperature-dependent part $\Delta\rho$ of the resistivity above the residual resistivity $\rho_0 = 0.17\,\mu\Omega$ cm is plotted for different conditions of pressure. **a**, $\Delta\rho$ on a quadratic temperature scale up to about 12 K and for pressures below the critical pressure, that is, in the ferromagnetic phase. As the Curie temperature is suppressed with pressure, the quadratic regime is observed only below about 6 K at 11.3 kbar. Inset, the cubic unit cell of the B20 lattice of MnSi. **b**, $\Delta\rho$ on a scale of $T^{3/2}$ up to about 6 K and for pressures above the critical pressure, that is, in the paramagnetic phase. From top to bottom, the pressures are 15.0, 18.1, 19.6, 25.3 and 27.5 kbar. The clear departure from a quadratic behaviour is shown in the inset for 15.0, 19.6 and 27.5 kbar.

with a disorder mean free path in excess of 5,000 Å (as confirmed by quantum oscillatory experiments[13] and by the low value of the residual resistivity ρ_0, which is 0.17 μΩ cm for the sample used here) suggests that disorder-related effects are not expected to interfere in the experimentally relevant temperature range. The Curie temperature and the transport properties of MnSi are highly sensitive to the application of hydrostatic pressure, and may be conveniently tuned using a conventional piston and cylinder cell. In particular, T_C falls monotonically with increasing pressure and vanishes at $p_c = 14.6$ kbar, the critical pressure of a zero-temperature phase transition. The continuous magnetic transition becomes first order when T_C is suppressed below about 12 K, that is, for pressures above 12 kbar (refs 14–17). Crucially, there is no singularity in the magnetic susceptibility at T_C as it tends to absolute zero, and therefore p_c cannot be classified as a strict quantum critical point[15–17].

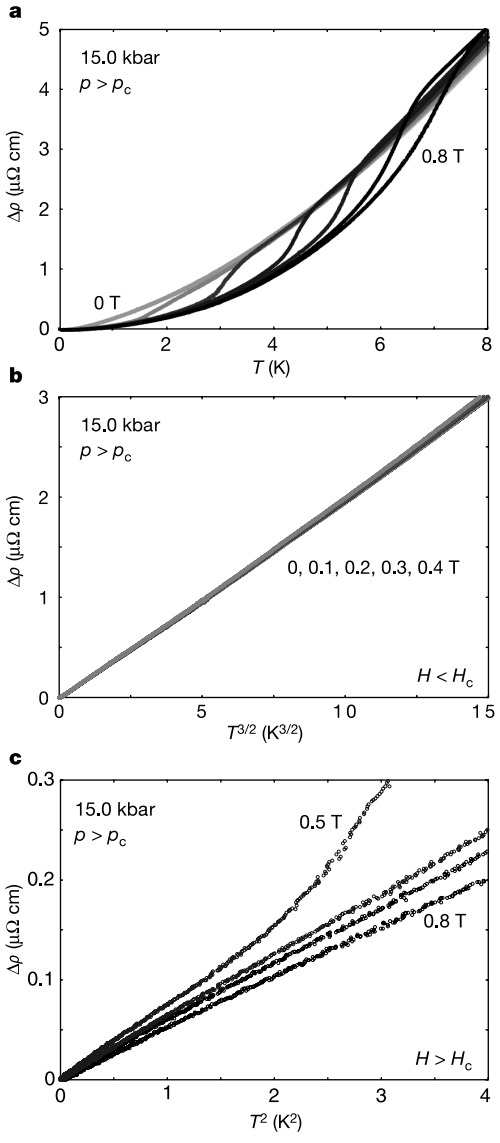

Figure 2 Dependence on temperature of the low-temperature resistivity of MnSi at 15.0 kbar and for different conditions of applied magnetic field. **a**, $\Delta\rho$ on a linear temperature scale up to 8 K. The curves shown are for 0, 0.1, 0.2, 0.3, 0.4, 0.5, 0.55, 0.6, 0.65, 0.7 and 0.8 T. For 0.4 T and below, the curves fall almost exactly on top of each other. The shoulder in the resistivity for 0.5 T and above signals a transition to a spin-polarized state at low temperatures, as known from magnetic susceptibility measurements[16]. The temperature associated with this transition increases with field. The zero-temperature critical field H_c associated with this field-induced ferromagnetic phase is between 0.4 and 0.5 T. **b**, $\Delta\rho$ on a scale of $T^{3/2}$ up to about 6 K and for 0, 0.1, 0.2, 0.3 and 0.4 T, that is, for $H < H_c$. **c**, $\Delta\rho$ on a scale of T^2 up to 2 K for 0.5, 0.6, 0.65 and 0.8 T, that is, for $H > H_c$. Above H_c and at low temperatures, the resistivity assumes a quadratic form similar to that seen in the zero-field ferromagnetic phase below p_c.

Here we report a high-precision study of the electrical resistivity of MnSi at pressures up to 27.5 kbar, nearly twice the critical pressure, and from room temperature down to typically 50 mK. Our main finding, shown in Figs 1 to 3, is the observation of a low-temperature electrical resistivity of the form $\rho = \rho_0 + AT^{3/2}$ in the paramagnetic phase above $p_c = 14.6$ kbar and up to the highest measured pressure of 27.5 kbar. Whereas the coefficient A is nearly halved over that pressure range (Fig. 1b), the exponent above p_c is weakly dependent on pressure and temperature and remains fixed at a value close to 3/2 (Fig. 3a). The quadratic exponent normally associated with a Fermi liquid is observed only when MnSi is in a spin-polarized state, either in the zero-field ferromagnetic phase at low pressures below p_c (Figs 1a and 3a), or in the field-induced ferromagnetic state above p_c (Figs 2c and 3b). We note that the range in resistivity $\Delta\rho$ over which an exponent close to 3/2 is observed is large compared to ρ_0, with the ratio $\Delta\rho/\rho_0$ in excess of 17 and 14 at 15.0 and 27.5 kbar, respectively. This suggests that the $T^{3/2}$ resistivity is an intrinsic property of the pure electronic system rather than the manifestation of the effect of impurities. In addition, this anomalous resistivity is found to be robust against at least an order of magnitude increase in ρ_0 near p_c (see Methods).

The observed resistivity exponent is in conflict with the quadratic behaviour expected in Fermi-liquid theory and thought to be applicable even near p_c at low temperatures in cases where the quantum phase transition is first order. The remarkable stability of this anomalous exponent from p_c up to nearly $2p_c$, and below a critical field, is unexpected: crucially, it suggests that at low temperatures MnSi may be described in terms of a conventional spin-polarized phase in which MnSi exhibits Fermi-liquid properties and a new paramagnetic phase characterized by a non-Fermi-liquid resistivity (Fig. 3d). This is expected to be followed at sufficiently high pressures by a conventional metallic phase (not yet seen). We interpret our observation as an unusual breakdown of the scheme normally associated with ferromagnetic quantum criticality in which only a narrow crossover regime, and not a phase, is predicted. It is in this crucial sense that the present work goes beyond—but is consistent with—the previous low-temperature studies of MnSi, which were restricted to pressures only in the immediate vicinity of p_c and below[10]. The extensive experimental and theoretical background of this system provides us with the means to quantify the degree to which this peculiar finding is in conflict with our current understanding.

Over the past several decades, the low-temperature properties of magnetic metals such as MnSi have been described with considerable success in terms of an extension of the Fermi-liquid model in which the magnetic interactions between quasiparticles are dominant and become long range in space and time as a quantum critical point is approached. This weakly or nearly ferromagnetic Fermi-liquid (NFFL) model leads to properties that may differ strikingly from that of a normal Fermi liquid, but strictly above a characteristic temperature T^* which vanishes only at the quantum critical point itself[18–22]. This crossover temperature T^* may be estimated in a simple way by examining the form of the relaxation frequency spectrum associated with spin fluctuations[18,23]. For an isotropic NFFL model, the natural rate of relaxation (Γ_q) for a spontaneous spin fluctuation of wavevector q in the paramagnetic state takes the form $\Gamma_q = \theta q(\xi^{-2} + q^2)$, where $\xi = (c\chi)^{1/2}$ is the magnetic correlation length, χ is the magnetic susceptibility, and θ and c are material-specific constants[23]. For the particular case of MnSi, this form for Γ_q is extensively supported by inelastic neutron scattering experiments[24].

The relaxation rate Γ_q is characterized by a linear term, $\theta q/\xi^2$, that represents Landau damping in a Fermi liquid, and a cubic term, θq^3,

that becomes progressively more important as the quantum critical point is approached and ξ diverges. These two components cross at a frequency θ/ξ^3 that turns out to measure the characteristic temperature $T^\star$ (if frequencies are expressed in temperature units). The breakdown of the conventional Fermi-liquid form of the resistivity may be expected to arise only for T, and thus frequencies, well above $T^\star$ where the relaxation rate is dominated by the cubic term. As the magnetic transition near p_c is first order, ξ is not expected to be very large in MnSi and therefore $T^\star$ is not expected to be very low (see below).

$T^\star$ can be estimated from (1) inelastic neutron scattering data[24] at ambient pressure that define the constants θ and c, and (2) bulk susceptibility measurements[15] as a function of temperature, magnetic field and pressure that, together with c, define ξ. For MnSi, we find $\theta \approx 600\,\mathrm{K\,\AA^3}$ and at p_c, $\xi \approx 6\,\mathrm{\AA}$ (ref. 23). This leads to an estimate of $T^\star$ of the order of 2 K and 10 K for pressures near p_c and $2p_c$, respectively. We stress that this estimate is in agreement with the results of direct numerical calculations of the temperature dependence of the resistivity based on the Boltzmann equation formalism[18]. Our estimate of $T^\star$ as a function of pressure up to $2p_c$ is represented by the dashed line in Fig. 4. So in the millikelvin range explored here (see Methods and Fig. 5), the NFFL model predicts a T^2 resistivity in essentially the entire experimental pressure and field region, in stark disagreement with our observations. This discrepancy becomes particularly difficult to ignore at the highest pressure studied here, where the non-Fermi-liquid form of the resistivity is observed down to temperatures over two orders of magnitude lower than $T^\star$.

In an attempt to understand our observations some issues may be raised, and here we briefly discuss two of them. First, the long-wavelength helical modulation of the ferromagnetic order is expected to lead to a modified relaxation rate of the form $\Gamma_q = \theta q(\xi^{-2} + q^2 - 2qQ)$, where Q is the wavevector of the helical modulation. But for MnSi, Q is $0.033\,\mathrm{\AA^{-1}}$ (ref. 12) and thus much smaller than $1/\xi$ in the paramagnetic state above p_c; that is, within the correlation length ξ the electrons are unaware of the helical modulation. This suggests that the latter leads in this case only to small corrections to the resistivity in our experimental range. In cases where Q and $1/\xi$ are comparable, however, the helical modulation may give rise to interesting and exotic behaviour (ref. 25 and M. Turlakov, personal communication).

Second, as for the effect of frozen-in disorder, the relevant length scale is the quasiparticle mean free path l. This is expected to lead to a modification of Γ_q for $q < 1/l$ and hence of the thermal properties for $T \leq \theta/(l\xi^2)$ (ref. 26). For the sample used here, this temperature scale is over three orders of magnitude smaller than $T^\star$ and therefore below the experimentally accessible range[13]. The conclusion on the ineffectiveness of disorder scattering for our pure sample is not greatly altered if we consider the relaxation rate associated with charge fluctuations rather than spin fluctuations[26]. We also note that the low values of ρ_0 both in the ferromagnetic and paramagnetic state and the weak dependence of $\Delta\rho$ on ρ_0 suggest that the $T^{3/2}$ resistivity cannot be explained in terms of frozen-in spin disorder due to the effect of impurities as in a conventional spin glass phase.

The theory of metals has thus far been based on the concept of elementary excitations, or in the context of the present problem, on magnetic fluctuations that are well behaved and in some sense

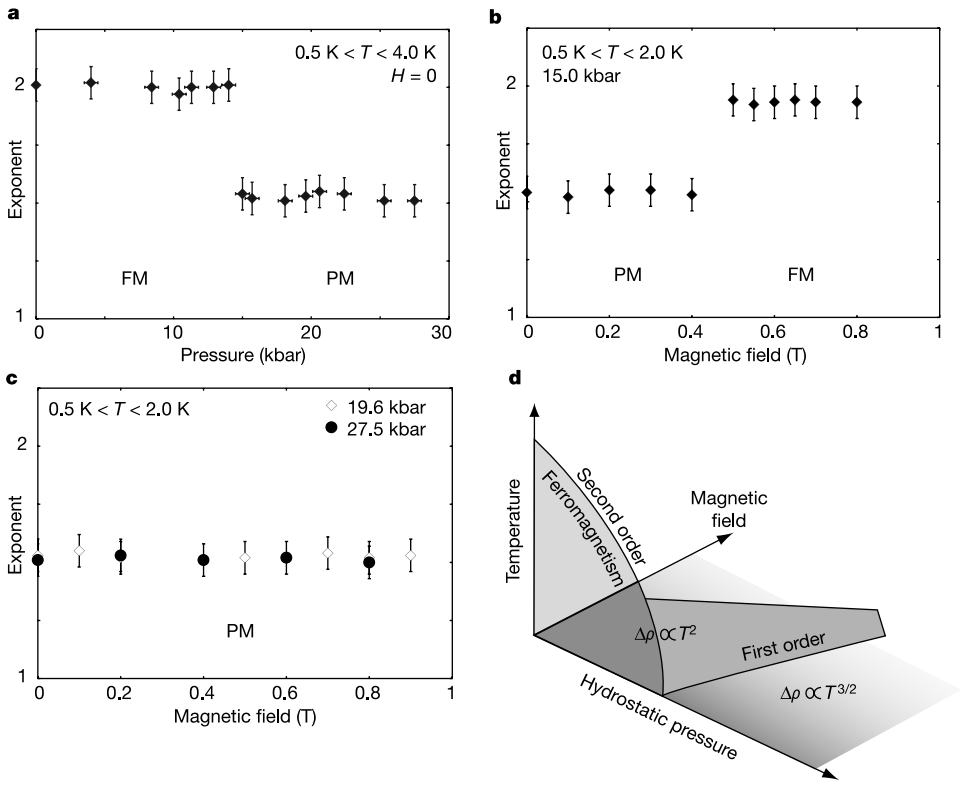

Figure 3 Low-temperature resistivity exponent as a function of pressure and magnetic field. The values are extracted from a least-squares fit to the resistivity data as a function of temperature. FM and PM denote the ferromagnetic and paramagnetic phases, respectively. **a**, Exponent as a function of pressure as observed between 0.5 and 4.0 K and in zero applied field. **b**, Exponent as a function of field as observed at 15.0 kbar between 0.5 and 2.0 K. For the data point at 0.5 T the range is 0.5 to 1.0 K because of the low transition temperature to the spin-polarized state (see Fig. 2c). **c**, Same as **b** but for 19.6 and 27.5 kbar where no spin polarization is observed in our experimental field range up to 0.9 T. Taken together, **a**–**c** may be seen as defining an anomalous phase in the temperature–pressure–magnetic field phase diagram with p_c and H_c for boundaries in the pressure–field plane. **d**, Illustration of the temperature–pressure–magnetic field phase diagram of MnSi supported by earlier studies[10,14–17,30] and by our findings. The details that arise from the helical structure have been omitted.

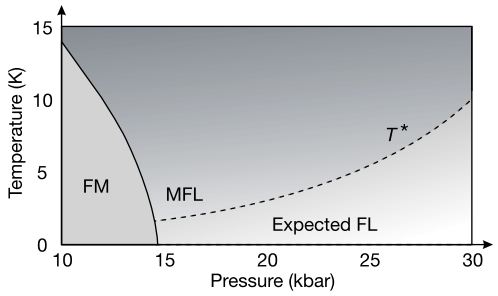

Figure 4 Illustration of the temperature-pressure phase diagram of MnSi predicted by the weakly or nearly ferromagnetic Fermi-liquid model (NFFL). In the ferromagnetic (FM) state at low temperatures and in the paramagnetic state below the crossover temperature T^*, the NFFL model reduces to the Fermi-liquid (FL) model characterized by a T^2 resistivity. Above T^* near the ferromagnetic boundary, the NFFL model reduces to the marginal Fermi-liquid (MFL) model described in our earlier work[10,15], which, in the ideal case of a continuous ferromagnetic transition where T^* vanishes, predicts a $T^{5/3}$ resistivity in the low-temperature limit[18]. In MnSi, however, the ferromagnetic transition is first order, and hence T^* remains finite at all pressures. In the ferromagnetic state and in the paramagnetic state above T^* or in high magnetic fields, the NFFL model provides a consistent quantitative description of the known properties of MnSi. Below T^* in the paramagnetic phase, however, our measurements conflict in a profound and crucial way with this phase diagram, in that no resistivity consistent with a Fermi-liquid description is observed anywhere below T^*, from p_c up to 27.5 kbar and down to 50 mK, that is, up to two orders of magnitude below T^*. We note that in calculating T^* we have assumed the parameters θ and c to be constants independent of temperature, magnetic field and pressure. We find, however, that within the NFFL model, no simple or plausible variation of these parameters can consistently account for the overall behaviour of the resistivity and of the magnetic susceptibility over the entire temperature, field and pressure ranges investigated.

smooth[1]. However, on the border of a first-order phase transition one might expect, in addition to these smooth fluctuations, the emergence of sudden large-amplitude fluctuations representing the spontaneous formation of droplets of local order. These highly anharmonic quantum and thermal fluctuations may not be described simply in terms of elementary excitations. Normally, such anharmonic fluctuations are frozen out by a high-energy barrier between the paramagnetic and locally ferromagnetic state, and lead to the well-known supercooling phenomenon and hysteresis associated with conventional first-order transitions[27]. In materials such as MnSi, however, the first-order transition may be weak enough to permit anharmonic fluctuations to play a new role in the quantum statistical mechanics of a metal at low temperature (T. V. Ramakrishnan and C. M. Varma, personal communication)[22].

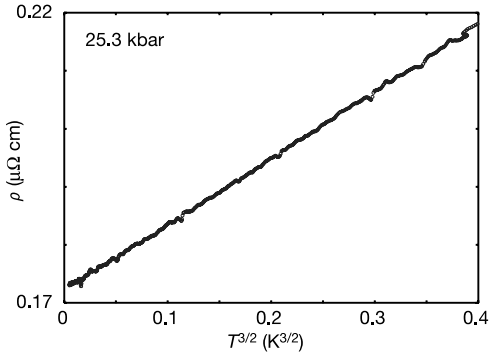

Figure 5 Dependence on temperature of the electrical resistivity of MnSi at subkelvin temperatures. In this range and for high-purity specimens, we have observed an exponent between 1.5 and 1.7. For this particular trace at 25.3 kbar and measured with a dilution refrigerator, ρ varies as $T^{3/2}$.

Evidence of anomalous behaviour on the border of first-order phase transitions that may support this view has recently been reported in other contexts[28]. The relevance of our findings in MnSi to other *d*-metal ferromagnets is the subject of several independent investigations (C. Pfleiderer, J. Flouquet, P. Niklowitz and D. Jaccard, personal communications). □

Methods

Samples

The single-crystal samples were grown by radio-frequency induction melting of zone-refined high-purity starting materials on a water-cooled copper crucible in an ultrahigh vacuum. The resulting ingots were annealed for two weeks near the melting point. Single-crystal samples were oriented by Laue X-ray diffraction, and cut to typically $2.0 \times 0.5 \times 0.5\ \mathrm{mm}^3$ using low-power spark erosion. Four electrical contacts were made immediately after etching the samples for 20 min in a solution of glycerol:HF:HCl:HNO_3 40:25:25:10. At ambient pressure, the elastic mean free path found in quantum oscillations measurements is in excess of 5,000 Å, in agreement with $\rho_0 = 0.17\ \mu\Omega\,\mathrm{cm}$.

Experimental procedure

The high-pressure experiment was performed using a 4-mm piston-and-cylinder clamp cell made exclusively of non-magnetic materials[29]. To achieve a high degree of hydrostaticity we employ as pressure medium an equal mix of *iso*-pentane and *n*-pentane known to remain liquid at room temperature in the experimentally relevant pressure range. The pressure cell is gold-plated for optimum thermal contact and to reduce the absorption of thermal radiation.

The use of ultra-low-noise a.c. detection based on cryogenically cooled electronics eliminates common problems related to, for example, thermal noise or drift effects, and allows measurements at very low excitation levels, even in the millikelvin range.

Measurements were performed and repeated on three different experimental systems, one conventional dilution refrigerator with a base temperature of 15 mK, and two demagnetization refrigerators reaching typically 50 mK. The slow sweep rate, of the order of $1\ \mathrm{mK\ min}^{-1}$ at low temperatures, ensures thermal equilibrium between the samples and the thermometry.

We stress that in the present work measurements were systematically performed on a number of samples and on all three experimental systems. Despite focusing here on the findings related to our purest sample, the observations reported here were also seen near p_c in samples of varying quality with residual resistivities as high as $2.4\ \mu\Omega\,\mathrm{cm}$.

Received 30 May; accepted 30 July 2003; doi:10.1038/nature01968.

1. Landau, L. D. *Collected Papers* (ed. Ter Haas, D.) Ch. 90, 91 (Pergamon, Oxford, 1965).
2. Murata, K. K. & Doniach, S. Theory of magnetic fluctuations in itinerant ferromagnets. *Phys. Rev. Lett.* **29,** 285–288 (1972).
3. Moriya, T. & Kawabata, A. Effect of spin fluctuations in itinerant electron ferromagnetism. *J. Phys. Soc. Jpn* **34,** 639–651 (1973).
4. Ramakrishnan, T. V. Microscopic theory of spin fluctuations in itinerant electron ferromagnets. *Phys. Rev. B* **10,** 4014–4024 (1974).
5. Hertz, J. A. Quantum critical phenomena. *Phys. Rev. B* **14,** 1165–1184 (1976).
6. Laughlin, R. B. *et al.* The quantum criticality conundrum. *Adv. Phys.* **50,** 361–365 (2001).
7. Anderson, P. W. In praise of unstable fixed points: The way things actually work. *Physica B* **318,** 28–32 (2002).
8. Schröder, A. *et al.*, Onset of antiferromagnetism in heavy-fermion metals. *Nature* **407,** 351–355 (2000).
9. Millis, A. J. Whither correlated electron theory? *Physica B* **312–313,** 1–6 (2002).
10. Pfleiderer, C., Julian, S. R. & Lonzarich, G. G. Non-Fermi-liquid nature of the normal state of itinerant-electron ferromagnets. *Nature* **414,** 427–430 (2001).
11. Bloch, D., Voiron, J., Jaccarino, V. & Wernick, J. H. The high field-high pressure magnetic properties of MnSi. *Phys. Lett.* **51,** 259–291 (1975).
12. Lebech, B. in *Recent Advances in Magnetism of Transition Metal Compounds* eds Kotani, A. & Suzuki, N.) 167–178 (World Scientific, Singapore, 1993).
13. Taillefer, L., Lonzarich, G. G. & Strange, P. The band magnetism of MnSi. *J. Magn. Magn. Mater.* **54–57,** 957–958 (1986).
14. Thompson, J. D., Fisk, Z. & Lonzarich, G. G. Perspective on heavy-electron and Kondo-lattice systems from high pressure studies. *Physica B* **161,** 317–323 (1989).
15. Pfleiderer, C., McMullan, G. J., Julian, S. R. & Lonzarich, G. G. Magnetic quantum phase transition in MnSi under hydrostatic pressure. *Phys. Rev. B* **55,** 8330–8338 (1997).
16. Thessieu, C. *et al.* Field dependence of the magnetic quantum phase transition in MnSi. *J. Phys. Condens. Matter* **9,** 6677–6687 (1997).
17. Thessieu, C., Ishida, K., Kitaoka, Y., Asayama, K. & Lapertot, G. Pressure effect on MnSi: An NMR study. *J. Magn. Magn. Mater.* **177–181,** 609–610 (1998).
18. Moriya, T. *Spin Fluctuations in Itinerant Electron Magnetism* (Springer, Berlin, 1985).
19. Millis, A. J. Effect of a non-zero temperature on quantum critical points in itinerant fermion systems. *Phys. Rev. B* **48,** 7183–7196 (1993).
20. Pfleiderer, C. Non-Fermi liquid puzzle of MnSi at high pressure *Physica B* **328** (1–2), 100–104 (2003).
21. Belitz, D., Kirkpatrick, T. R., Narayanan, R. & Vojta, T. Transport anomalies and marginal-Fermi-liquid effects at a quantum critical point. *Phys. Rev. Lett.* **85,** 4602–4605 (2000).
22. Varma, C. M., Nussinov, Z. & van Saarloos, W. Singular or non-Fermi liquids. *Phys. Lett.* **361,** 267–417 (2002).
23. Lonzarich, G. G. & Taillefer, L. Effect of spin fluctuations on the magnetic equation of state of ferromagnetic or nearly ferromagnetic metals. *J. Phys. C* **18,** 4339–4371 (1985).
24. Ishikawa, Y., Noda, Y., Uemura, Y. J., Majkrzak, C. F. & Shirane, G. Paramagnetic spin fluctuations in the weak itinerant-electron ferromagnet MnSi. *Phys. Rev. B* **31,** 5884–5893 (1985).

25. Vojta, T. & Sknepnek, R. Quantum phase transition of itinerant helimagnets. *Phys. Rev. B* **64,** 052404 (2001).
26. Altshuler, B. L. & Aronov, A. G. in *Electron-Electron Interactions in Disordered Systems* (eds Pollak, M. & Efros, A. L.) 1–153 (Modern Problems in Condensed Matter Sciences, North Holland, Amsterdam, 1985).
27. Langer, J. S. Statistical theory of the decay of metastable states. *Ann. Phys.* **54,** 258–275 (1969).
28. Rivadulla, F., Zhou, J.-S. & Goodenough, J. B. Electron scattering near an itinerant to localized electronic transition. *Phys. Rev. B* **67,** 165110 (2003).
29. Walker, I. R. Nonmagnetic piston-cylinder pressure cell for use at 35 kbar and above. *Rev. Sci. Instrum.* **70,** 3402–3412 (1999).
30. Yamada, H. & Terao, K. Itinerant-electron metamagnetism of MnSi at high pressure. *Phys. Rev. B* **59,** 9342–9347 (1999).
31. Custers, J. *et al.*, The break-up of heavy electrons at a quantum critical point. *Nature* **424,** 524–527 (2003).

Acknowledgements We thank the following for discussions; B. Altshuler, S. Barakat, S. Brown, P. Coleman, J. Flouquet, R. K. W. Haselwimmer, D. Khmelnistkii, A. J. Millis, P. Monthoux, P. Niklowitz, C. Pfleiderer, T. V. Ramakrishnan, S. S. Saxena, B. Simon, M. Turlakov and C. M. Varma. The work was supported by the UK EPSRC and the EU FERLIN programme. N.D.-L. acknowledges support from FCAR of Quebec, NSERC of Canada, and Trinity College and Peterhouse, Cambridge University.

Competing interests statement The authors declare that they have no competing financial interests.

Correspondence and requests for materials should be addressed to N.D.-L. (nd223@cam.ac.uk).

Temperature-induced valence transition and associated lattice collapse in samarium fulleride

J. Arvanitidis[1], Konstantinos Papagelis[1], Serena Margadonna[2], Kosmas Prassides[1] & Andrew N. Fitch[3]

[1]*Department of Chemistry, University of Sussex, Brighton BN1 9QJ, UK*
[2]*Department of Chemistry, University of Cambridge, Cambridge CB2 1EW, UK*
[3]*European Synchrotron Radiation Facility, 38042 Grenoble, France*

The different degrees of freedom of a given system are usually independent of each other but can in some materials be strongly coupled, giving rise to phase equilibria sensitively susceptible to external perturbations. Such systems often exhibit unusual physical properties that are difficult to treat theoretically, as exemplified by strongly correlated electron systems such as intermediate-valence rare-earth heavy fermions and Kondo insulators, colossal magnetoresistive manganites and high-transition temperature (high-T_c) copper oxide superconductors. Metal fulleride salts[1]—metal intercalation compounds of C_{60}—and materials based on rare-earth metals also exhibit strong electronic correlations. Rare-earth fullerides thus constitute a particularly intriguing system—they contain highly correlated cation (rare-earth) and anion (C_{60}) sublattices. Here we show, using high-resolution synchrotron X-ray diffraction and magnetic susceptibility measurements, that cooling the rare-earth fulleride $Sm_{2.75}C_{60}$ induces an isosymmetric phase transition near 32 K, accompanied by a dramatic isotropic volume increase and a samarium valence transition from $(2+\epsilon)+$ to nearly 2+. The negative thermal expansion—heating from 4.2 to 32 K leads to contraction rather than expansion—occurs at a rate about 40 times larger than in ternary metal oxides typically exhibiting such behaviour[2]. We attribute the large negative thermal expansion, unprecedented in fullerene or other molecular systems, to a quasi-continuous valence transition from Sm^{2+} towards the smaller $Sm^{(2+\epsilon)+}$, analogous to the valence or configuration transitions encountered in intermediate-valence Kondo insulators like SmS (ref. 3).

The transition between superconducting and antiferromagnetic insulating behaviour of C_{60}-based fullerides is sensitively controlled by the ratio (U/W) between the on-site Coulomb repulsion energy, U, and the conduction bandwidth, W (ref. 1). Whereas intense efforts in the last decade have exhaustively mapped the electronic and superconducting properties of intercalated alkali and alkaline-earth fullerides[4–6], little is known about the electronic properties of other metal fullerides, especially those of rare-earth elements, Ln, which present the possibility of strong coupling between two electronically active sublattices, $\pi(C_{60})$ and $4f,5d$(Ln). The most prominent examples of rare-earth fullerides are the $Yb_{2.75}C_{60}$ ($T_c = 6$ K)[7] and $Sm_{2.75}C_{60}$ ($T_c = 8$ K)[8] superconductors, whose complex orthorhombic structures are related to those of primitive cubic sodium fullerides[9] and arise from the long-range ordered arrangement of tetrahedral rare-earth metal vacancies, accompanied by orientational ordering of C_{60} units about local three-fold symmetry rotational axes[7].

First, we found no evidence in $Sm_{2.75}C_{60}$ for a transition to a superconducting state down to 2 K in contrast to ref. 8 and in agreement with other explorations of the Sm–C_{60} phase field[10]. We then probed the temperature evolution of the structural properties of the $Sm_{2.75}C_{60}$ fulleride by high-resolution synchrotron X-ray diffraction, and examined the diffraction profiles collected over a restricted angular range of 3.3° to 25° (d-spacing, 13.9 to 1.85 Å) at various temperatures between 4.2 and 295 K. Inspection of the diffraction profiles readily reveals the appearance of superlattice peaks at low angles that index to the enlarged orthorhombic unit cell (space group *Pcab*) proposed before[7,11]. However, a striking feature of the data is that the diffraction peaks at low temperatures continuously shift to higher angles on heating, implying an anomalous structural behaviour whereby the material rapidly contracts as the temperature increases above 4.2 K (Fig. 1). The trend is reversed above 32 K and normal behaviour is restored with the lattice smoothly expanding on heating to 295 K. Besides the shifts in peak positions, no changes in relative peak intensities are apparent in the diffraction profiles throughout the whole temperature range, implying the absence of a phase transition to a structure with

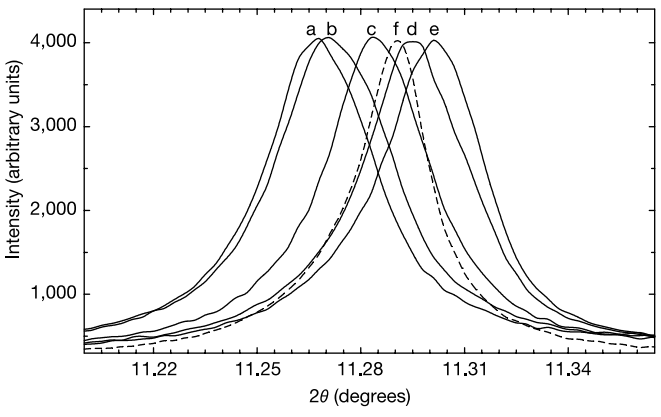

Figure 1 Selected region of the diffraction profile of $Sm_{2.75}C_{60}$ showing the temperature evolution of the (444) Bragg reflection ($\lambda = 0.79980$ Å). Trace a, 4.2 K; b, 10 K; c, 16 K; d, 21 K; e, 32 K; and f, 200 K. The peak shifts monotonically to higher angles (lattice contraction) on heating from 4.2 to 32 K and then to lower angles (lattice expansion) on further heating to room temperature. Its width remains essentially constant in the temperature range in which the negative thermal expansion is observed. Then it sharpens continuously on heating to 150 K (by ~45%) with little further change to room temperature. Such behaviour could reflect the presence of a structural phase transition undetectable even with the ultrahigh resolution of the present measurements. More likely it could be the signature of precursor effects to the valence transition and the existence of local structural inhomogeneities accompanying the transformation.